

Unifying Synergies between Self-supervised Learning and Dynamic Computation

Tarun Krishna¹ Ayush K. Rai¹ Alexandru Drimbarean² Alan F. Smeaton¹ Kevin McGuinness¹
Noel E. O'Connor¹

Abstract

Self-supervised learning (SSL) approaches have made major strides forward by emulating the performance of their supervised counterparts on several computer vision benchmarks. This, however, comes at a cost of substantially larger model sizes, and computationally expensive training strategies, which eventually lead to larger inference times making it impractical for resource constrained industrial settings. Techniques like *knowledge distillation* (KD), *dynamic computation* (DC), and *pruning* are often used to obtain a *lightweight* sub-network, which usually involves multiple epochs of fine-tuning of a large pre-trained model, making it more computationally challenging.

In this work we propose a novel perspective on the interplay between SSL and DC paradigms that can be leveraged to simultaneously learn a *dense* and *gated* (sparse/lightweight) *sub-network* from scratch offering a good accuracy-efficiency trade-off, and therefore yielding a generic and multi-purpose architecture for application specific industrial settings. Our study overall conveys a constructive message: exhaustive experiments on several image classification benchmarks: CIFAR-10, STL-10, CIFAR-100, and ImageNet-100, demonstrates that the proposed training strategy provides a *dense* and corresponding *sparse* sub-network that achieves comparable (on-par) performance compared with the vanilla self-supervised setting, but at a significant reduction in computation in terms of FLOPs under a range of target budgets.

1. Introduction

Motivation. Self-supervised representation learning methods (Chen et al., 2020a; Caron et al.; Chen et al.; Chen

& He; Bardes et al.) are the new norms for training large scale deep neural networks (DNNs). Their ability to exploit the underlying structure of the data from a large unlabelled corpus during pre-training makes them a preferred choice for transfer learning (Goyal et al., 2021). Pre-training not only helps with better transferability but also leads to better generalization on various downstream tasks compared to supervised pretraining. This ability, however, comes at the cost of substantially larger model size, computationally expensive training strategies (larger training times, large batch-sizes, etc.) (Chen et al., 2020b; Goyal et al., 2021), and accordingly more expensive inference times. Such strategies prove effective in achieving *state-of-the-art* (SOTA) results on several downstream tasks in computer vision but are impractical under resource (memory, power and compute) constrained *industrial* settings, where major emphasis is given on deploying a lightweight model on edge devices.

A common practice to reduce this computational burden is to extract a lightweight sub-network¹ from an off-the-shelf pre-trained model, or pre-training the model as a part of a multi-step training process and further compressing it by applying techniques like Knowledge distillation (KD) (Hinton et al., 2015), pruning (Frankle & Carbin, 2018), dynamic computation (DC) (Veit & Belongie, 2018), etc. SSL based pre-training combined with KD² (Tian et al., 2019; Abbasi Koohpayegani et al., 2020; Fang et al., 2021), DC (Krishna et al., 2022; Meng et al., 2022), or pruning (Caron et al., 2020; Chen et al., 2021) also serve as effective ways to obtain a lightweight sub-network for a given downstream task. This sequential learning procedure often involves fine-tuning a pre-trained self-supervised model on a downstream task along with the corresponding training objective of KD, DC, or pruning with cross entropy (CE) loss. This works, but obtaining a sub-network from large pre-trained models (e.g. large language models (LLMs)) via fine-tuning makes the overall process computationally more expensive and cumbersome. Furthermore, downstream tasks are diverse and vary widely; therefore, any change in the downstream task usually requires repeating the entire procedure multiple

¹Insight Centre for Data Analytics, Dublin City University, Dublin, Ireland ²Xperi Corporation. Correspondence to: Tarun Krishna <tarun.krishna2@mail.dcu.ie>.

¹A network derived from another large model/network

²For clarification in KD a different lightweight network (not sub-network) is learnt.

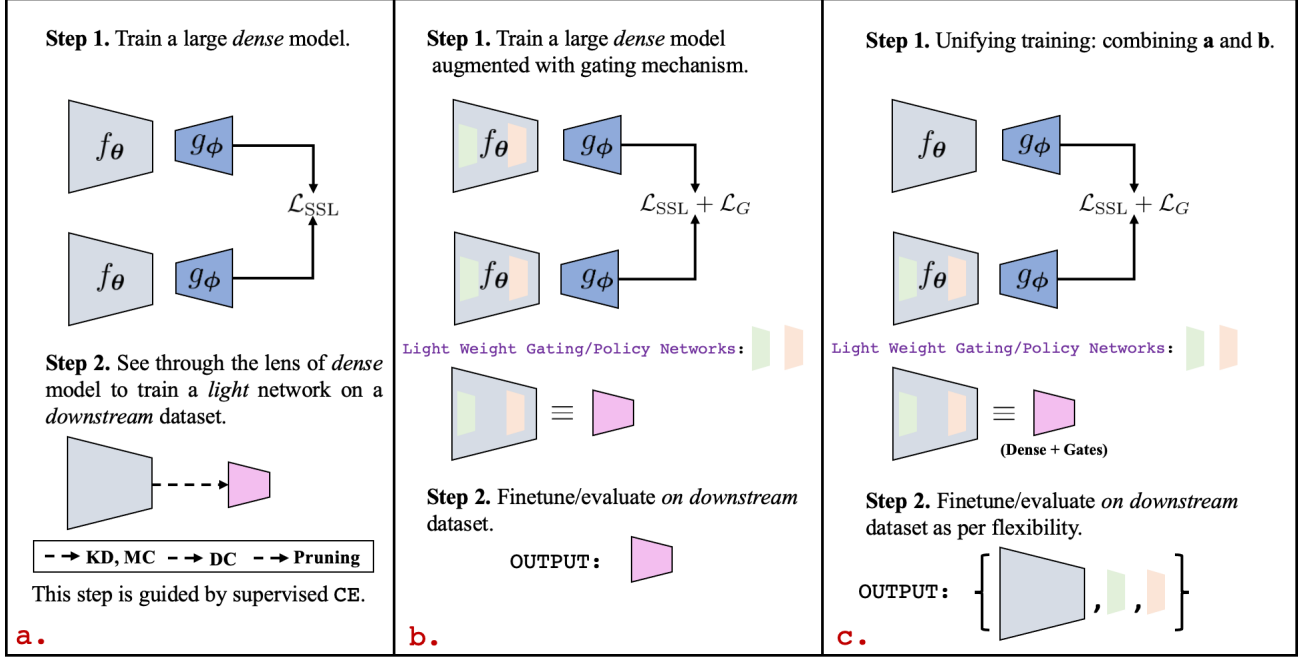


Figure 1. This figure illustrates different settings; **a.** Shows the general setting for achieving a lightweight sub-network/small-network following different techniques. **b.** More relevant to this work, illustrates the setting showcased in (Krishna et al., 2022) but modified as per our use case (i.e, instead of SimSiam(Chen & He, 2021) we use VICReg objective). **c.** This work: we learn a dense encoder and some gates based on a budget constraint t_d . With this gating mechanism the dense encoder can be exploited as a lightweight sub-network as well as dense network. Here **b** and **c** are based on gating mechanisms introduced in (Veit & Belongie, 2018; Li et al., 2021). Figure best viewed in color.

times, making it highly inefficient and less transferable.

Research Questions. These limitations compel us to ask the following question: • “Can we unify the learning of a lightweight sub-network along with a dense network from scratch and in a completely self-supervised fashion?” In other words, by the end of a pre-training procedure one has access to a dense and a lightweight sub-network simultaneously, saving not only time obtaining the sub-network after pre-training, but also giving flexibility to exploit both the dense and the lightweight network as per the use case. Instead of fine-tuning a large model to get a lightweight network one can directly work on lightweight sub-network directly after pre-training. Having said that, our focus is on faster inference however we intend to achieve this by not adding too much computational overhead during training. This leads us to reformulate the research question to: • “Can we learn an encoder (function) that could serve the dual purpose of being used as a dense and lightweight network with minimal additional overhead?” Our goal is to simultaneously learn a dense and a lightweight model under a single training procedure. In Figure 1c we demonstrate the dual setting of obtaining a dense and a lightweight network (derived from dense). Mathematically, given an encoder f_{θ} and gating functions \mathbf{W} then a sub-network $\mathcal{S}(\mathbf{x}) = f_{\theta}(\mathbf{x}, \mathbf{W} \odot \theta)$, where \mathbf{W} can be interpreted as learning a mask at differ-

ent levels in the network (Figure 3 in Appendix A.3). For obtaining \mathbf{W} we follow dynamic channel selection (DCS) (Veit & Belongie, 2018; Li et al., 2021) to induce sparsity while maintaining network topology. Figure 1a depicts the traditional setting alternating between pre-training and fine-tuning while Figure 1b depicts the setting recently introduced in (Krishna et al., 2022) using dynamic channel selection along with self-supervision. Also from now on, lightweight, sub-network or gated network refer to same thing.

The lightweight network can be interpreted as *student* while dense network as the *teacher* where the *teacher* is as bad as (initially un-trained) the *student*. Note that in this work we do not follow the vocabulary of teacher-student networks. Instead we restrict the terminology to lightweight (Gated) and a dense network, where encoder and gates³ are randomly initialised and trained jointly from scratch, with an aim that they co-evolve during training. It is, however, important to mention that in this work we are not proposing any new KD objective or KD induced learning algorithm nor any new DC objective neither any pruning based learning. Instead we provide a novel perspective on exploiting the synergies that exist between self-supervised

³encoder with gates \equiv sub-network depicted very clearly in Figure 1c

representation learning and dynamic computing. In addition to the teacher-student paradigm, this work also takes inspiration from SDCLR (Jiang et al., 2021) and APPRENTICE (Mishra & Marr, 2017), which exploit a joint student-teacher KD based approach for very specific applications.

To this end we focus on joint embedding symmetric-siamese architecture specifically VICReg (Bardes et al.) architecture amalgamated with dynamic channel selection (Veit & Belongie, 2018; Li et al., 2021). Below we outline our main contributions:

- We present a novel perspective of unifying the learning of *dense* and *lightweight* networks by exploiting a symmetric joint embedding architecture of the SSL paradigm.
- We demonstrate that a single encoder can be exploited as a dense as well as a lightweight network, we show in Table 1 and Table 2 that a single base encoder can serve this dual purpose. This not only reduces computational overhead during training but also gives enough flexibility to use a single network and exploit it as per its requirement.
- We exhaustively, through experiments, demonstrate that this unification preserves feature quality across different experimental settings and gives on-par performance when compared with strict baselines (Section 4).

2. Related Works

2.1. Self-supervised Visual Representation Learning

SSL has recently matched the performance of supervised learning on several computer vision benchmarks (Chen et al., 2020a; Caron et al.; Chen et al.; Chen & He; Grill et al., 2020; Hjelm et al., 2018; Wu et al., 2018b; Asano et al., 2019). At the core of these approaches is the concept of learning joint embedding representations realised via a Siamese (Chopra et al., 2005) architecture through instance discrimination. Most of the design choices of SSL methods are formulated in a way to avoid *feature collapse*⁴. Broadly, these SSL methods can be divided into contrastive and non-contrastive techniques. Contrastive learning (Wu et al., 2018b; Oord et al., 2018; Hénaff et al., 2020; Chen et al., 2020a; He et al., 2020; Tian et al., 2020; Le-Khac et al., 2020) based approaches intuitively try to bring similar instances closer in the embedding space while contrasting them with negative samples. Non-contrastive techniques includes clustering methods (Caron et al., 2018; Asano et al., 2019), which alternate between cluster assignment and predicting clusters as pseudo labels, which make them computationally cumbersome as they require running a clustering

step over the entire dataset. SwAV (Caron et al.) mitigates this computationally expensive step by making the clustering completely online. Approaches like BYOL (Grill et al., 2020), OBoW (Gidaris et al., 2020), and SimSiam (Chen & He, 2021) avoid using contrastive samples or clustering, exploiting tricks like a “momentum encoder” or applying a “stop-gradient” operator in one branch (Chen & He, 2021). However, why and how these techniques avoid collapse is still unclear and an open research area. A more principled way of learning representations while avoiding feature collapse relies on information maximization; examples include: Barlow Twins (Zbontar et al., 2021), W-MSE (Ermolov et al.), and VICReg (Bardes et al.). In this work we exploit one of the key property of VICReg i.e., *independent* branch regularization which works better in scenarios where representation in each branch has different statistics, so the amount of regularization required for each branch may vary a lot, though this property seems to be under utilized in the SSL domain.

2.2. Dynamic Computation (DC)

DC is an effective, adaptive, and resource efficient computing mechanism to reduce model complexity by skipping unimportant parts of network depending on the input. Several authors including (Figurnov et al., 2017; McGill & Perona, 2017; Huang et al., 2018; Wu et al., 2020; Wang et al., 2018) have proposed adding decision branches to different layers of convolutional neural networks (CNN) for learning early exiting strategies leading to faster inference. Block-Drop (Wu et al., 2018a) and SpotTune (Guo et al., 2019) learn a policy network to adaptively route the inference path through fine-tuned or pre-trained layers. ConvNet-AIG (Veit & Belongie, 2018), (Herrmann et al., 2020) introduced a network that adaptively selects specific layers of importance to execute depending on the input image by specifying a target rate of each layer. GaterNet (Chen et al., 2019) introduced a network to generate input-dependent binary gates to select filters in the backbone network. CGNet (Hua et al., 2019) exploits spatial diversity to allocate different computation for different activations while DGNet (Li et al., 2021) proposed a dual gating mechanism to induce sparsity along spatial and channel dimensions. Furthermore, dynamic channel pruning methods have also been devised such as feature boosting and suppression (FBS) (Gao et al., 2019) to dynamically amplify and suppress output channels computed by CNN layers. Other works learn sparsity through a three-stage pipeline: *pretrain-prune-finetune* as in (Tiwari et al., 2020) or use pre-trained models. See (Hoeffler et al., 2021) for a more detailed explanation of sparsity, pruning, and dynamic computing. In this work we use the dynamic channel selection mechanism proposed in (Veit & Belongie, 2018; Li et al., 2021).

⁴dimensional collapse, information collapse

2.3. Self-supervised Dynamic Computation and Beyond

Most of the works on dynamic computation have been mostly confined to supervised learning. Recently, (Krishna et al., 2022) used SimSiam (Chen & He) as a self-supervised objective combined with a dynamic channel gating (DGNet) (Li et al., 2021) mechanism *trained from scratch*, and showed that comparable performance can be achieved under channel budget constraints. Likewise (Meng et al., 2022) used a channel gating-based dynamic pruning (CGNet) (Hua et al., 2019) augmented with contrastive learning to achieve inference speed-ups without substantial loss of performance. Similarly, (Caron et al., 2020) showed that the performance of the pruned sub-network is maintained on the pretext task, which is further maintained after being transferred to a downstream task. In a similar line of work, (Chen et al., 2021) used iterative magnitude pruning (IMP) to obtain a winning ticket (Frankle & Carbin, 2018) for a pre-trained task (self-supervised objective) and evaluated its performance on various downstream tasks. (Pan et al., 2022) extended the work done in (Caron et al., 2020) in a MoCo (pre-trained) setting augmented with ADMM (Zhang et al., 2018) for systematic pruning. A self-supervised *loss* objective can serve as a tool for knowledge distillation (KD) (Hinton et al., 2015) and model compression (MC). (Tian et al., 2019) used contrastive objective (along with supervised loss *task specific distillation*) to train a student network from pre-trained network. Similar to (Tian et al., 2019) but in a completely self-supervised setting (Abasi Koohpayegani et al., 2020; Fang et al., 2021) minimizes *KL*-divergence between the distribution of similarities for teacher (pre-trained) and student networks. The authors in (Xu et al., 2020) used a two-step strategy to train teacher (learn with labels and then learn SSL head with fixed backbone) followed by learning student using KD loss. However, we follow a more simplistic approach through unification of SSL (VICReg) and DCS where DCS adds more flexibility as compared to pruning (or KD) by maintaining network topology and making the fine-tuning process convenient on various downstream tasks while for later approaches it's irreversible (network structure).

3. Preliminaries and Setups

3.1. Method

VICReg. Based on the principle of *information maximization*, VICReg (Bardes et al.) learns a joint embedding space governed by a loss objective which comprises of *invariance* (s) (mean squared error (MSE)), *variance* (v) and *co-variance* (c) as shown in Equation 1. Assume an image dataset $\mathcal{D} = \{\mathbf{x}_1, \dots, \mathbf{x}_{|\mathcal{D}|}\}$, where $\mathbf{x}_i \in \mathbb{R}^{3 \times H \times W}$ with empirical probability distribution $p(\mathbf{X})$ and a set of transformations \mathcal{T} (see Appendix A for details). An anchor image $\mathbf{x}_i \sim p(\mathbf{X})$ (or a batch \mathcal{B}) and corresponding

two transformations t_1 and t_2 are sampled from \mathcal{T} to get $\mathbf{x}_i^1 = t_1(\mathbf{x}_i)$ and $\mathbf{x}_i^2 = t_2(\mathbf{x}_i)$, augmented views of \mathbf{x}_i . \mathbf{x}_1 and \mathbf{x}_2 are encoded through f_θ (ResNet-18 (He et al., 2016) in this study) to get *representations* $f_\theta(\mathbf{x}_i^1)$ and $f_\theta(\mathbf{x}_i^2)$ respectively. Furthermore, these representations are mapped to an *embedding* space via *expander* g_ϕ where the final VICReg loss is applied between the embedding vectors $\mathbf{z}_i^1 = g_\phi(f_\theta(\mathbf{x}_i^1))$ and $\mathbf{z}_i^2 = g_\phi(f_\theta(\mathbf{x}_i^2))$ (or a batch of embedding vectors $\mathbf{Z}^1 = [\mathbf{z}_1^1, \dots, \mathbf{z}_{|\mathcal{B}|}^1]$ and $\mathbf{Z}^2 = [\mathbf{z}_1^2, \dots, \mathbf{z}_{|\mathcal{B}|}^2]$). Formally the loss is defined as⁵:

$$\mathcal{L}_{\text{VICReg}}(\mathbf{Z}^1, \mathbf{Z}^2) = \underbrace{\mu[v(\mathbf{Z}^1) + v(\mathbf{Z}^2)]}_{\text{Variance}} + \underbrace{\nu[c(\mathbf{Z}^1) + c(\mathbf{Z}^2)]}_{\text{Co-Variance}} + \underbrace{\eta s(\mathbf{Z}^1, \mathbf{Z}^2)}_{\text{Invariance}}, \quad (1)$$

where $\mu = 25$, $\nu = 25$ and $\eta = 1.0$. For a more elaborate description of different loss term please refer (Bardes et al.).

Dynamic Channel Gating. Channel selection (or conditional computation) adapts the network to different inputs while keeping the architecture fixed (Han et al., 2021; Veit & Belongie, 2018; Li et al., 2021). Given an input \mathbf{x}_{l-1} (output from a previous layer), the output from a static network (or a module: A block in ResNet) is given by $\mathbf{x}_l = f_\theta(\mathbf{x}_{l-1}, \theta)$ while a network (module) equipped with dynamic computation will be represented by $\mathbf{y} = f_\theta(\mathbf{x}_{l-1}, \hat{\theta})$ such that $\hat{\theta} = \mathcal{W}(\mathbf{x}_{l-1}, \theta, \omega)$ where $\omega \in \{\mathbf{w}_1, \mathbf{w}_2\}$. \mathcal{W} can be thought of as a lightweight policy network to decide the *importance*⁶ vector for a given input feature map \mathbf{x}_{l-1} , which is crucial in order to avoid trivial solutions. The most common and effective technique to realize \mathcal{W} is via *squeeze and excitation* blocks (Hu et al., 2018). This usually requires obtaining a context vector $\mathbf{z} \in \mathbb{R}^{C_{l-1}}$ via global average pooling to accumulate spatial information. Consequently, this context vector \mathbf{z} is passed through \mathcal{W} which is composed of:

$$\mathcal{W}(\mathbf{x}_{l-1}, \theta, \omega) = \mathbf{w}_2(\text{norm}(\mathbf{w}_1 \mathbf{z}))_+, \quad (2)$$

where $+$ is ReLU operation, norm denotes batch norm layer, $\mathbf{w}_1 \in \mathbb{R}^{\frac{C_{l-1}}{r} \times C_l}$, $\mathbf{w}_2 \in \mathbb{R}^{C_l \times \frac{C_{l-1}}{r}}$ and r is defined as reduction rate (set to 4). $\mathbf{w}_1, \mathbf{w}_2$ are realised through convolutional layer. Finally, in order to achieve $\hat{\theta}$, binary selection is applied on $\mathcal{W}(\mathbf{x}_{l-1}, \theta, \omega)$ (`torch.where` ($\mathcal{W} \geq 0.5, 1, 0$)) to get a binary mask $m \in \mathbb{R}^{C_l}$ such that $\hat{\theta} = \theta \odot m$. This discrete selection works perfectly during inference but breaks the computational graph during training. To make training feasible the Gumbel-softmax trick (Jang et al., 2016) is adopted. The Gumbel-Trick has been widely used as a reparameterisation technique for the task of dynamic

⁵Notations same as (Bardes et al.)

⁶also known as saliencies/relevance/attention

channel selection (Krishna et al., 2022; Li et al., 2021; Hermann et al., 2020; Veit & Belongie, 2018). For more clarity refer Figure 4 in Appendix A.3. In this work we closely follow the setting of DGNet (Li et al., 2021) for channel selection where sparsity is induced by setting a global target budget (t_d) to optimize a loss objective defined as:

$$\mathcal{L}_G = \lambda \left(\frac{\sum_{l=1}^L F_l^R}{\sum_{l=1}^L F_l^O} - t_d \right)^2, \quad (3)$$

where F_l^R is the average FLOPs over the batch along with FLOPs computation lightweight \mathcal{W} network, while F_l^O is the original FLOPs without a gating module with $\lambda = 5$ (Li et al., 2021) across all datasets and training regimes. Only blocks with gating modules take part in FLOP computation as they are responsible for introducing sparsity in the network. Refer Figure 4 in Appendix A.3.

Final Loss. The overall training objective is defined as: $\mathcal{L} = \mathcal{L}_{\text{VICReg}} + \mathcal{L}_G$.

3.2. Experimental Setup and Implementation Details

3.2.1. PRE-TRAINING

We closely follow the implementation of VICReg (Bardes et al.) (as our self-supervised objective) suited with our computational constraints using solo-learn library (da Costa et al., 2022), while for dynamic gating we follow DGNet (Li et al., 2021) for inducing channel sparsity via gating mechanism with ResNet18 (modified basic blocks Figure 3 in Appendix A.3) (*single* network) as the base encoder as depicted in Figure 1c, also the two branches have separate batch normalization layer following (Yu et al., 2019). The encoder is *randomly* initialized and trained with SGD for 500 epochs with a batch size of 256 on 2 Nvidia 2080Ti GPUs, with a warmup start of 10 epochs following a cosine decay with a base learning rate of 0.3 using LARS optimizer (You et al., 2017). Since we are using a very lightweight model as our gating network, there is no significant computational overhead during training. We report the inference speedup in terms of hardware-independent theoretical metric of FLOPs and not wall-clock time as we are not using any hardware accelerators to utilise sparsity during training. Note: we do not perform any hyper-parameter search and most of the choices are based on computational availability. Any scaling parameter involved in the loss term is derived from respective papers. A Pytorch-style pseudocode is also provided in Appendix A.2.

3.2.2. EVALUATION

Pre-training and evaluation is carried on the train and validation data of CIFAR-10/100 (Krizhevsky et al., 2009), ImageNet100 (taken from here) and STL-10 (Coates et al., 2011). For pre-training with STL-10 we considered

only the *un-labelled* set. We pre-train for a target budget, $t_d = \{10\%, 20\%, 30\%, 40\%, 50\%\}$ for each of the datasets except for ImageNet-100 where t_d is restricted to $\{30\%, 40\%, 50\%\}$ due to computational constraints.

For evaluating the learned representation we follow the standard practice of evaluating the trained encoder by freezing its weights and training a linear classifier on top of it. We trained a single linear layer for 100 epochs with a batch size of 512 on a single NVIDIA 2080Ti with a learning rate of 0.3 following step decay of 0.1 at 60th and 80th epochs. This strategy is followed across all datasets. We report top-1 accuracy averaged over 5 runs. We also use k -nearest neighbours (kNN) as our evaluation metric with $k = 1$ for ablations.

To exhaustively compare the performance of the dense and gated models we consider VICReg (Bardes et al.) as a SSL *dense* baseline while VICReg augmented with sparsity loss as in Equation 3 (following (Krishna et al., 2022)) serves as a *gated* baseline.

4. Results

1. Quantitative assessment. Table 1 compares the performance of VICReg-Dual-Gating with the other two baselines for dense and gated. The lightweight gated network achieves improved performance across all datasets and target budgets (t_d) as compared to *Baseline-2* (Figure 1b), with a negligible drop at $t_d = 50\%$ for CIFAR-10 only. The improved gated performance can be attributed to the fact that both dense and gated models co-learn during training via weight sharing. However, the performance gain is compensated by a slightly smaller reduction in FLOPs as compared to *Baseline-2*. Improved performance of gated network further closes the gap with a completely self-supervised dense model (*Baseline-1*). With only 10% of the target budget, the gated network achieves accuracy on-par with the *Baseline-1* and even surpasses the performance on CIFAR-100 for $t_d = 40\%$. Performance is comparable for all the other datasets across different t_d . In comparison to *Baseline-1*, we observe a drop in performance of VICReg-Dual-Gating e.g., at $t_d = 10\%$ across CIFAR-10 ($\downarrow 2.17\%$), STL-10 ($\downarrow 2.86\%$), CIFAR-100 ($\downarrow 1.55\%$), ImageNet-100 ($\downarrow 2.7\%$) but at a significant reduction in number of FLOPs. This illustrates that even under severe budget constraint our model achieves comparable performance to *Baseline-1*. This drop further decreases on increasing t_d to 50%.

Another important aspect of our learning method is performance of the dense model. Ideally one would aim to achieve fewer fluctuations with varying t_d with a performance equivalent to dense model as in *Baseline-1*. However, we find that the performance of the dense network (*this work*) is slightly below the performance of the dense (*Baseline-1*)

Table 1. Linear Evaluation: Here we compare the performance of VICReg-Dual with two baselines VICReg and VICReg-Gating (VICReg modified following (Krishna et al., 2022)) respectively. \uparrow/\downarrow in orange font is comparison with *Baseline-1*, while blue font is comparison with *Baseline-2*. FLOPs R. denotes FLOP reduction. We report Top-1 accuracy averaged over 5 runs. Best viewed in color.

Dataset	VICReg Baseline-1 (Bardes et al.)		$t_d(\%)$	VICReg-Gating Baseline-2 (Krishna et al., 2022)		VICReg-Dual <i>this work</i>		
	Dense	FLOPs		Gated	FLOPs R.	Dense \uparrow	Gated \uparrow	FLOPs R. \uparrow
CIFAR-10	91.11 \pm 0.03	7.03E8	10%	87.75 \pm 0.03	85.92%	88.99 \pm 0.04 (\downarrow 2.12)	88.94 \pm 0.06 (\downarrow 2.17) (\uparrow 1.19)	81.49% (\downarrow 4.43)
			20%	88.00 \pm 0.04	78.03%	89.68 \pm 0.05 (\downarrow 1.43)	89.44 \pm 0.01 (\downarrow 1.67) (\uparrow 1.44)	74.36% (\downarrow 3.67)
			30%	89.49 \pm 0.04	69.27%	90.38 \pm 0.04 (\downarrow 0.73)	90.27 \pm 0.03 (\downarrow 0.84) (\uparrow 0.78)	66.43% (\downarrow 2.84)
			40%	89.87 \pm 0.03	61.10%	90.46 \pm 0.05 (\downarrow 0.65)	90.10 \pm 0.03 (\downarrow 1.01) (\uparrow 0.23)	57.53% (\downarrow 3.57)
			50%	90.70 \pm 0.04	51.62%	90.20 \pm 0.02 (\downarrow 0.91)	90.40 \pm 0.06 (\downarrow 0.71) (\downarrow 0.30)	49.02% (\downarrow 2.60)
STL-10	86.15 \pm 0.10	3.33E8	10%	82.48 \pm 0.15	82.85%	84.29 \pm 0.21 (\downarrow 1.86)	83.29 \pm 0.05 (\downarrow 2.86) (\uparrow 0.81)	78.34% (\downarrow 4.51)
			20%	82.90 \pm 0.21	76.35%	84.52 \pm 0.12 (\downarrow 1.63)	84.32 \pm 0.02 (\downarrow 1.83) (\uparrow 1.42)	72.21% (\downarrow 4.14)
			30%	84.16 \pm 0.11	68.38%	84.90 \pm 0.05 (\downarrow 1.25)	84.85 \pm 0.04 (\downarrow 1.30) (\uparrow 0.69)	65.24% (\downarrow 3.14)
			40%	84.90 \pm 0.10	58.89%	85.43 \pm 0.15 (\downarrow 0.72)	84.90 \pm 0.07 (\downarrow 1.25) (\uparrow 0.00)	57.11% (\downarrow 1.78)
			50%	85.40 \pm 0.20	49.93%	85.75 \pm 0.02 (\downarrow 0.40)	85.72 \pm 0.02 (\downarrow 0.43) (\uparrow 0.32)	48.41% (\downarrow 1.52)
CIFAR-100	65.86 \pm 0.10	7.03E8	10%	63.12 \pm 0.09	84.82%	65.21 \pm 0.06 (\downarrow 0.65)	64.31 \pm 0.08 (\downarrow 1.55) (\uparrow 1.19)	81.71% (\downarrow 3.11)
			20%	64.64 \pm 0.01	77.25%	66.10 \pm 0.05 (\uparrow 0.24)	65.82 \pm 0.03 (\downarrow 0.04) (\uparrow 1.18)	74.94% (\downarrow 2.31)
			30%	65.41 \pm 0.09	68.68%	65.90 \pm 0.10 (\uparrow 0.04)	65.64 \pm 0.00 (\downarrow 0.22) (\uparrow 0.23)	66.83% (\downarrow 1.85)
			40%	65.71 \pm 0.04	60.60%	67.07 \pm 0.16 (\uparrow 1.21)	66.70 \pm 0.05 (\uparrow 0.89) (\uparrow 0.99)	57.99% (\downarrow 2.61)
			50%	65.75 \pm 0.12	50.04%	66.41 \pm 0.05 (\uparrow 0.55)	66.40 \pm 0.14 (\uparrow 0.54) (\uparrow 0.65)	49.06% (\downarrow 0.98)
ImageNet-100	77.74 \pm 0.12	1.81E9	30%	74.04 \pm 0.09	67.95%	75.12 \pm 0.07 (\downarrow 2.62)	75.04 \pm 0.10 (\downarrow 2.17) (\uparrow 1.00)	64.98% (\downarrow 2.97)
			40%	75.61 \pm 0.04	59.55%	76.45 \pm 0.03 (\downarrow 1.29)	76.13 \pm 0.20 (\downarrow 1.61) (\uparrow 1.00)	56.41% (\downarrow 3.14)
			50%	75.83 \pm 0.07	50.11%	76.42 \pm 0.26 (\downarrow 1.32)	76.24 \pm 0.12 (\downarrow 1.51) (\uparrow 0.41)	47.69% (\downarrow 2.42)

Table 2. Transfer Performance: dense and gated under VICReg-Dual is compared with the common dense *baseline* of VICReg. \uparrow/\downarrow represents increment/decrement in performance. We report Top-1 linear evaluation accuracy averaged over 5 runs.

Dataset	VICReg (Bardes et al.) Dense	VICReg-Dual							
		10%		20%		30%		40%	
From \rightarrow To		Dense	Gated	Dense	Gated	Dense	Gated	Dense	Gated
CIFAR-100 \rightarrow STL-10	70.37	64.69 \downarrow	64.29 \downarrow	65.02 \downarrow	65.69 \downarrow	65.63 \downarrow	65.93 \downarrow	66.73 \downarrow	66.90 \downarrow
CIFAR-100 \rightarrow CIFAR-10	80.08	80.56 \uparrow	79.92 \downarrow	80.00 \downarrow	79.95 \downarrow	80.23 \uparrow	80.24 \uparrow	80.79 \uparrow	80.65 \uparrow
CIFAR-100 \rightarrow ImageNet-100	39.45	35.88 \downarrow	36.31 \downarrow	38.56 \downarrow	38.97 \downarrow	38.49 \downarrow	38.20 \downarrow	38.05 \downarrow	38.69 \downarrow
ImageNet-100 \rightarrow STL-10	72.80	-	-	-	-	65.86 \downarrow	65.01 \downarrow	66.96 \downarrow	67.09 \downarrow
ImageNet-100 \rightarrow CIFAR-10	55.12	-	-	-	-	53.38 \downarrow	49.41 \downarrow	53.42 \downarrow	50.14 \downarrow
ImageNet-100 \rightarrow CIFAR-100	31.42	-	-	-	-	28.81 \downarrow	25.55 \downarrow	27.41 \downarrow	25.24 \downarrow

for CIFAR-10/STL-10/ImageNet-100 while for CIFAR-100 the performance is better than the self-supervised dense module. This is interesting because what we achieve from this single experiment of 500 training epochs is a single base encoder (dense encoder) and gates (gating modules) and their combination gives a gated lightweight network which is equivalent to running two separate experiments as reported in Table 1 under VICReg and VICReg-Gating.

2. Transfer Learning. Table 2 compares the transfer performance of VICReg-Dual (dense and gated) with VICReg. This experiment gives further insights into the quality of the learned representation in this joint setting. In general, there is a drop in performance for VICReg-Dual for both *dense* and *gated*, although the difference is not significant. However, for CIFAR-100 \rightarrow CIFAR-10 *dense* and *gated* outperforms only *dense* in VICReg at a very low target budget. Even in the case when the model is pre-trained on ImageNet-100, performance is comparable. This is encouraging as this new perspective still maintains good generalization and

transferability. *Note* the encoder was frozen and was linearly evaluated following the protocol as in Section 3.2.2.

3. Qualitative assessment. Figure 2 shows uniform manifold approximation and projection (UMAP) (McInnes et al., 2018) embeddings of the learned representation ($f_\theta(\mathbf{x}) \in \mathbb{R}^{512}$) trained using dual-setting on the STL-10 dataset and compares it with VICReg (Bardes et al.). The learned structure is similar to dense (VICReg) at a very low budget. Along with that the classes appear to be visually distinct, similar to the VICReg setting, and this is observed for both the dense and gated networks of VICReg-Dual.

5. Auxiliary Insights and Ablation Study

For all experimental settings and studies from now on; models (and settings) were pre-trained for 500 epochs on CIFAR-100 and STL-10 datasets. Instead of using linear evaluation we use kNN as the evaluation criterion with $k = 1$ to report *top-1* accuracy. In results table from now on **bold** and

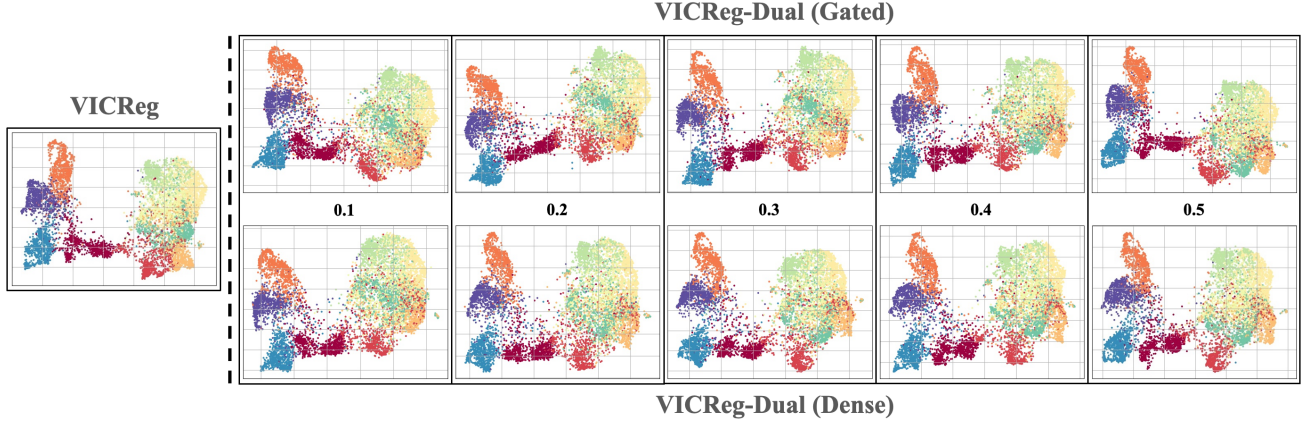


Figure 2. **Qualitative analysis:** The top row displays UMAP embeddings of the learned representations through the *lightweight* network while the *bottom* row displays the dense model over different target budgets t_d . This is compared with embeddings of VICReg (dense) trained without any sort of sparsity. Best viewed in color. Note: $\{0.1, 0.2, 0.3, 0.4, 0.5\}$ refers to $\{10\%, 20\%, 30\%, 40\%, 50\%\}$ t_d .

Table 3. Symmetric architecture: BT vs VICReg in dual setting (kNN-1 as evaluation metric).

Dataset	t_d	BT-Dual			VICReg-Dual		
		Dense	Gated	FLOPs R.	Dense	Gated	FLOPs R.
CIFAR-100	10%	53.64	53.01	80.60%	54.92	<u>54.66</u>	<u>81.71%</u>
	20%	54.33	53.88	74.56%	55.97	<u>55.86</u>	<u>74.94%</u>
	30%	55.03	54.89	66.09%	56.34	<u>55.53</u>	<u>66.83%</u>
	40%	55.26	55.04	57.34%	56.66	<u>56.44</u>	<u>57.98%</u>
	50%	55.63	55.39	47.64%	56.83	<u>57.25</u>	<u>49.06%</u>
STL-10	10%	73.45	73.49	76.74%	76.61	<u>76.45</u>	<u>78.27%</u>
	20%	74.89	74.81	69.68%	77.45	<u>77.70</u>	<u>72.16%</u>
	30%	75.51	76.02	64.12%	78.55	<u>78.80</u>	<u>65.17%</u>
	40%	76.90	75.93	57.14%	79.01	<u>78.85</u>	<u>57.05%</u>
	50%	76.99	77.10	48.32%	79.69	<u>79.95</u>	<u>48.39%</u>

Table 4. Different encoder: Single vs Double base encoder (kNN-1 as evaluation metric).

Dataset	t_d (%)	VICReg-Dual (1×ResNet-18)			VICReg-Dual (2×ResNet-18)		
		Dense	Gated	FLOPs R.	Dense	Gated	FLOPs R.
CIFAR-100	10%	54.92	<u>54.66</u>	81.71%	53.85	52.44	<u>85.77%</u>
	20%	55.97	<u>55.86</u>	74.94%	54.78	54.30	<u>77.63%</u>
	30%	56.34	<u>55.53</u>	66.83%	55.65	55.52	<u>70.07%</u>
	40%	56.66	<u>56.44</u>	57.98%	55.54	55.40	<u>61.05%</u>
	50%	56.83	<u>57.25</u>	49.06%	55.64	55.71	<u>52.60%</u>
STL-10	10%	76.61	<u>76.45</u>	78.27%	74.93	74.89	<u>82.48%</u>
	20%	77.45	<u>77.70</u>	72.16%	76.10	75.29	<u>76.51%</u>
	30%	78.55	<u>78.80</u>	65.17%	76.83	76.71	<u>69.26%</u>
	40%	79.01	<u>78.85</u>	57.05%	77.73	77.08	<u>60.00%</u>
	50%	79.69	<u>79.95</u>	48.39%	77.74	78.00	<u>51.10%</u>

underline are the best performing attributes for dense and gated module respectively.

1. Comparison with symmetric architecture Barlow Twins (BT). VICReg is build upon the findings of BT (Zbontar et al., 2021) and it is straightforward to also apply the dual setting in BT because it again minimizes the cross-correlation (regularization term) to identity \mathcal{I} although the loss function is entirely mutual unlike in VICReg. In Table 3 we compare the performance of BT augmented with *our* setting. We observe that kNN performance for BT is low as

Table 5. Investigating role of MSE (kNN-1 as evaluation metric).

Dataset	t_d (%)	VICReg-Dual w/ Invariance			VICReg-Dual w/o Invariance		
		Dense	Gated	FLOPs R.	Dense	Gated	FLOPs R.
CIFAR-100	10%	54.92	<u>54.66</u>	81.71%	4.06	6.31	<u>93.77%</u>
	20%	55.97	<u>55.86</u>	74.94%	3.72	6.02	<u>86.45%</u>
	30%	56.34	<u>55.53</u>	66.83%	4.84	4.89	<u>82.72%</u>
	40%	56.66	<u>56.44</u>	57.98%	4.11	3.36	<u>68.26%</u>
	50%	56.83	<u>57.25</u>	49.06%	2.79	4.15	<u>49.05%</u>
STL-10	10%	76.61	<u>76.45</u>	78.27%	11.79	18.02	<u>90.71%</u>
	20%	77.45	<u>77.70</u>	72.16%	11.79	20.81	<u>82.45%</u>
	30%	78.55	<u>78.80</u>	65.17%	12.25	17.89	<u>74.96%</u>
	40%	79.01	<u>78.85</u>	57.05%	11.59	17.25	<u>66.51%</u>
	50%	79.69	<u>79.95</u>	48.39%	12.81	15.72	<u>51.91%</u>

compared to VICReg-Dual. The drop in performance could be attributed to the fact that VICReg applies independent regularisation and further regularised representations are matched through invariance loss (MSE).

2. Training with different base encoder. In this setting we train a model with two base encoders, one w/ gate (gated) and other w/o gate (dense) i.e. $(2 \times \text{ResNet-18})$ (results in Table 4). An interesting observation is that VICReg-Dual with a single base encoder performs better than a more powerful setting with two base encoders (Table 4) although FLOPs Reduction (FLOPs R.) is more (\uparrow) in the setting of two different encoders. This is due to the fact that sparsity loss (\mathcal{L}_G) operates solely on the un-shared branch so there is no trade-off involved as in case of single base encoder which simultaneously tries to enforce sparsity and visual invariance.

3. Role of mean squared error in co-evolving. It’s a well know fact in SSL that these methods suffer from dimension collapse (Hua et al., 2021; Jing et al.). Training without any regularization term or any trick (Grill et al., 2020; Chen & He, 2021) would lead to dimensional collapse. Also, authors in (Kim et al., 2021) showed that MSE serves as a better option for exact logit matching as compared to Kullback-

Table 6. Evaluation of different training settings (kNN-1 as evaluation metric).

Dataset	$t_d(\%)$	VICReg-Dual (Vanilla)			+Separate.bn			+Warmup-epochs		
		Dense	Gated	FLOPs Red.	Dense	Gated	FLOPs Red.	Dense	Gated	FLOPs Red.
CIFAR-100	10%	54.05	55.14	81.57%	54.92	54.66	81.71%	55.59	55.38	79.61%
	20%	54.81	55.71	73.98%	55.97	55.86	74.94%	55.22	55.12	72.39%
	30%	55.79	<u>56.33</u>	66.27%	56.34	55.53	<u>66.83%</u>	55.64	55.67	66.19%
	40%	56.11	<u>57.15</u>	57.72%	56.66	56.44	<u>57.99%</u>	55.87	55.80	57.36%
	50%	56.01	<u>56.57</u>	49.03%	56.83	57.25	49.06%	56.06	56.13	49.26%
STL-10	10%	76.50	76.53	<u>78.70%</u>	76.49	76.25	78.34%	77.53	<u>77.44</u>	73.20%
	20%	77.01	76.91	<u>72.33%</u>	77.41	77.59	72.21%	78.04	<u>78.14</u>	68.11%
	30%	78.10	77.85	<u>65.26%</u>	78.49	78.54	65.24%	78.79	<u>78.80</u>	62.62%
	40%	78.70	78.71	56.84%	79.14	78.84	<u>57.11%</u>	79.35	<u>79.04</u>	55.36%
	50%	79.68	79.85	48.36%	79.76	79.95	<u>48.41%</u>	79.89	<u>80.00</u>	47.35%

Leibler (KL) divergence. So, in order to understand the role MSE we trained a model w/o *invariance* loss. As depicted in Table 5 we found that there is huge performance drop if we get rid of invariance term. This implies invariance term plays a crucial role and seem to be an important factor not only for co-evolving but for self-supervision as well.

4. Effect of batch statistics and warm-up period during training. In this ablation study, we evaluate different training settings (different batch statistics and warm-up period) to find best performance and computational trade-off as highlighted in Table 6. For clarification, here warm-up refers to the number of epochs (10 epochs in this study) for which the model was trained without any sort of sparsity loss (no gating) which is different from the one used in optimization in Section 3.2.1. In Table 6, *Vanilla* refers to the setting where we introduce gates at different levels and sparsity loss to the original VICReg (Bardes et al.), while *Separate_BN* refers to extending *Vanilla* setting by having different batch normalization layers as batch statistics would vary for the sparse and dense branch (Yu et al., 2019; Jiang et al., 2021). Finally, this setting is extended by training for 10 epochs without any sparsity loss (and gates) under *Warm-up period* in Table 6. Overall the setting with *Separate_BN* offers best trade-off for accuracy and flops reduction.

6. Discussion and Conclusion

In this work we proposed a novel perspective on unifying synergies between self-supervised learning and dynamic computing essential for industrial applications. We exploit adaptive computing to induce sparsity into symmetric branches of self-supervised models enabling both branches to co-evolve with each other during training. In addition, this approach also allows simultaneous training of a dense and gated (sparse) sub-network from scratch with a target budget t_d under a self-supervised training objective with minimal computational overhead via weight sharing therefore offering a good accuracy-efficiency trade-off for a given

downstream application. As a result, our single base encoder offers enough flexibility to serve a dual purpose to reduce excessive computational overhead as illustrated in Table 1 and Table 2.

However, there are limitations with this work. Firstly, dense model seems to under-perform and it’s performance further fluctuates with varying t_d . However, we tried RotNet (Gidaris et al., 2018) as a extra proxy loss for dense branch but it didn’t yield good performance. Secondly, we haven’t imposed any constraint in the training objective that enforces uniform distribution of channel activations i.e. preservation of channel diversity during inference (could be a solution for our first limitation). Also, it will also be interesting to study channel activation distribution for different classes to further build an intuition about the approach. Thirdly, in future we would like to extend this setting to contrastive approaches and non-symmetric architectures as well.

We would like to reiterate that our goal is to demonstrate that when self-supervised learning is combined with adaptive computing, it results in a flexible dual purpose framework. This work is an initial attempt to draw parallels and make an inter-connection between both of these fields. However, more steps need to be taken in this direction to build a better intuition behind these models and also help us understand their other attributes such as generalization and ability to transfer to other downstream tasks.

References

- Abbasi Koohpayegani, S., Tejankar, A., and Pirsiavash, H. Compress: Self-supervised learning by compressing representations. *Advances in Neural Information Processing Systems*, 33:12980–12992, 2020. 1, 4
- Asano, Y. M., Rupprecht, C., and Vedaldi, A. Self-labelling via simultaneous clustering and representation learning. *arXiv preprint arXiv:1911.05371*, 2019. 3
- Bardes, A., Ponce, J., and Lecun, Y. VICReg: Variance-Invariance-Covariance Regularization for Self-

- Supervised Learning. Technical report. 1, 3, 4, 5, 6, 8, 12
- Caron, M., Misra, I., Mairal, J., Goyal, P., Bojanowski, P., and Joulin, A. Unsupervised Learning of Visual Features by Contrasting Cluster Assignments. Technical report. URL <https://github.com/facebookresearch/swav>. 1, 3
- Caron, M., Bojanowski, P., Joulin, A., and Douze, M. Deep clustering for unsupervised learning of visual features. In *Proceedings of the European conference on computer vision (ECCV)*, pp. 132–149, 2018. 3
- Caron, M., Morcos, A., Bojanowski, P., Mairal, J., and Joulin, A. Pruning convolutional neural networks with self-supervision. *arXiv preprint arXiv:2001.03554*, 2020. 1, 4
- Chen, T., Research, G., Luo, C., and Li, L. Intriguing Properties of Contrastive Losses. 1, 3
- Chen, T., Kornblith, S., Norouzi, M., and Hinton, G. A Simple Framework for Contrastive Learning of Visual Representations. 2020a. URL <http://arxiv.org/abs/2002.05709>. 1, 3
- Chen, T., Kornblith, S., Swersky, K., Norouzi, M., and Hinton, G. E. Big self-supervised models are strong semi-supervised learners. *Advances in neural information processing systems*, 33:22243–22255, 2020b. 1
- Chen, T., Frankle, J., Chang, S., Liu, S., Zhang, Y., Carbin, M., and Wang, Z. The lottery tickets hypothesis for supervised and self-supervised pre-training in computer vision models. In *Proceedings of the IEEE/CVF Conference on Computer Vision and Pattern Recognition*, pp. 16306–16316, 2021. 1, 4
- Chen, X. and He, K. Exploring Simple Siamese Representation Learning. Technical report. 1, 3, 4
- Chen, X. and He, K. Exploring simple siamese representation learning. In *Proceedings of the IEEE/CVF Conference on Computer Vision and Pattern Recognition*, pp. 15750–15758, 2021. 2, 3, 7
- Chen, Z., Li, Y., Bengio, S., and Si, S. You look twice: Gatnet for dynamic filter selection in cnns. In *Proceedings of the IEEE/CVF Conference on Computer Vision and Pattern Recognition*, pp. 9172–9180, 2019. 3
- Chopra, S., Hadsell, R., and LeCun, Y. Learning a similarity metric discriminatively, with application to face verification. In *2005 IEEE Computer Society Conference on Computer Vision and Pattern Recognition (CVPR'05)*, volume 1, pp. 539–546 vol. 1, 2005. doi: 10.1109/CVPR.2005.202. 3
- Coates, A., Ng, A., and Lee, H. An analysis of single-layer networks in unsupervised feature learning. In *Proceedings of the fourteenth international conference on artificial intelligence and statistics*, pp. 215–223. JMLR Workshop and Conference Proceedings, 2011. 5
- da Costa, V. G. T., Fini, E., Nabi, M., Sebe, N., and Ricci, E. solo-learn: A library of self-supervised methods for visual representation learning. *J. Mach. Learn. Res.*, 23: 56–1, 2022. 5
- Ermolov, A., Siarohin, A., Sangineto, E., and Sebe, N. Whitening for Self-Supervised Representation Learning. Technical report. 3
- Fang, Z., Wang, J., Wang, L., Zhang, L., Yang, Y., and Liu, Z. Seed: Self-supervised distillation for visual representation. *arXiv preprint arXiv:2101.04731*, 2021. 1, 4
- Figurnov, M., Collins, M. D., Zhu, Y., Zhang, L., Huang, J., Vetrov, D., and Salakhutdinov, R. Spatially adaptive computation time for residual networks. In *Proceedings of the IEEE conference on computer vision and pattern recognition*, pp. 1039–1048, 2017. 3
- Frankle, J. and Carbin, M. The lottery ticket hypothesis: Finding sparse, trainable neural networks. In *International Conference on Learning Representations*, 2018. 1, 4
- Gao, X., Zhao, Y., Dudziak, L., Mullins, R., and Cheng-Zhong, X. Dynamic channel pruning: Feature boosting and suppression. <https://iclr.cc/Conferences/2019>, 2019. 3
- Gidaris, S., Singh, P., and Komodakis, N. Unsupervised representation learning by predicting image rotations. *arXiv preprint arXiv:1803.07728*, 2018. 8
- Gidaris, S., Bursuc, A., Puy, G., Komodakis, N., Cord, M., and Pérez, P. Online bag-of-visual-words generation for unsupervised representation learning. *arXiv preprint arXiv:2012.11552*, 2020. 3
- Goyal, P., Caron, M., Lefaudeaux, B., Xu, M., Wang, P., Pai, V., Singh, M., Liptchinsky, V., Misra, I., Joulin, A., et al. Self-supervised pretraining of visual features in the wild. *arXiv preprint arXiv:2103.01988*, 2021. 1
- Grill, J.-B., Strub, F., Altché, F., Tallec, C., Richemond, P., Buchatskaya, E., Doersch, C., Avila Pires, B., Guo, Z., Gheshlaghi Azar, M., et al. Bootstrap your own latent—a new approach to self-supervised learning. *Advances in neural information processing systems*, 33:21271–21284, 2020. 3, 7

- Guo, Y., Shi, H., Kumar, A., Grauman, K., Rosing, T., and Feris, R. Spottune: transfer learning through adaptive fine-tuning. In *Proceedings of the IEEE/CVF conference on computer vision and pattern recognition*, pp. 4805–4814, 2019. 3
- Han, Y., Huang, G., Song, S., Yang, L., Wang, H., and Wang, Y. Dynamic neural networks: A survey. *IEEE Transactions on Pattern Analysis and Machine Intelligence*, 2021. 4
- He, K., Zhang, X., Ren, S., and Sun, J. Deep residual learning for image recognition. In *Proceedings of the IEEE conference on computer vision and pattern recognition*, pp. 770–778, 2016. 4, 12
- He, K., Fan, H., Wu, Y., Xie, S., and Girshick, R. Momentum contrast for unsupervised visual representation learning. In *Proceedings of the IEEE/CVF conference on computer vision and pattern recognition*, pp. 9729–9738, 2020. 3
- Hénaff, O. J., Srinivas, A., De Fauw, J., Razavi, A., Doersch, C., Eslami, S. M. A., and Van Den Oord, A. Data-Efficient Image Recognition with Contrastive Predictive Coding. Technical report, 2020. 3
- Herrmann, C., Bowen, R. S., and Zabih, R. Channel selection using gumbel softmax. In *European Conference on Computer Vision*, pp. 241–257. Springer, 2020. 3, 5
- Hinton, G., Vinyals, O., Dean, J., et al. Distilling the knowledge in a neural network. *arXiv preprint arXiv:1503.02531*, 2(7), 2015. 1, 4
- Hjelm, R. D., Fedorov, A., Lavoie-Marchildon, S., Grewal, K., Bachman, P., Trischler, A., and Bengio, Y. Learning deep representations by mutual information estimation and maximization. *arXiv preprint arXiv:1808.06670*, 2018. 3
- Hoefler, T., Alistarh, D., Ben-Nun, T., Dryden, N., and Peste, A. Sparsity in deep learning: Pruning and growth for efficient inference and training in neural networks. *Journal of Machine Learning Research*, 22(241):1–124, 2021. 3
- Hu, J., Shen, L., and Sun, G. Squeeze-and-excitation networks. In *Proceedings of the IEEE conference on computer vision and pattern recognition*, pp. 7132–7141, 2018. 4
- Hua, T., Wang, W., Xue, Z., Ren, S., Wang, Y., and Zhao, H. On feature decorrelation in self-supervised learning. In *Proceedings of the IEEE/CVF International Conference on Computer Vision*, pp. 9598–9608, 2021. 7
- Hua, W., Zhou, Y., De Sa, C., Zhang, Z., and Suh, G. E. Channel gating neural networks. In *Proceedings of the 33rd International Conference on Neural Information Processing Systems*, pp. 1886–1896, 2019. 3, 4
- Huang, G., Chen, D., Li, T., Wu, F., van der Maaten, L., and Weinberger, K. Multi-scale dense networks for resource efficient image classification. In *International Conference on Learning Representations*, 2018. 3
- Jang, E., Gu, S., and Poole, B. Categorical reparameterization with gumbel-softmax. *arXiv preprint arXiv:1611.01144*, 2016. 4, 12
- Jiang, Z., Chen, T., Mortazavi, B. J., and Wang, Z. Self-damaging contrastive learning. In *International Conference on Machine Learning*, pp. 4927–4939. PMLR, 2021. 3, 8
- Jing, L., Vincent, P., Lecun, Y., and Tian, Y. UNDERSTANDING DIMENSIONAL COLLAPSE IN CONTRASTIVE SELF-SUPERVISED LEARNING. 7
- Kim, T., Oh, J., Kim, N., Cho, S., and Yun, S.-Y. Comparing kullback-leibler divergence and mean squared error loss in knowledge distillation. *arXiv preprint arXiv:2105.08919*, 2021. 7
- Krishna, T., Rai, A. K., Djilali, Y. A., Smeaton, A. F., McGuinness, K., and O’Connor, N. E. Dynamic channel selection in self-supervised learning. *arXiv e-prints*, pp. arXiv–2207, 2022. 1, 2, 4, 5, 6
- Krizhevsky, A., Hinton, G., et al. Learning multiple layers of features from tiny images. 2009. 5
- Le-Khac, P. H., Healy, G., and Smeaton, A. F. Contrastive representation learning: A framework and review. *IEEE Access*, 8:193907–193934, 2020. doi: 10.1109/ACCESS.2020.3031549. 3
- Li, F., Li, G., He, X., and Cheng, J. Dynamic dual gating neural networks. In *Proceedings of the IEEE/CVF International Conference on Computer Vision (ICCV)*, pp. 5330–5339, October 2021. 2, 3, 4, 5, 12
- McGill, M. and Perona, P. Deciding how to decide: Dynamic routing in artificial neural networks. In *International Conference on Machine Learning*, pp. 2363–2372. PMLR, 2017. 3
- McInnes, L., Healy, J., and Melville, J. Umap: Uniform manifold approximation and projection for dimension reduction. *arXiv preprint arXiv:1802.03426*, 2018. 6

- Meng, J., Yang, L., Shin, J., Fan, D., and Seo, J.-S. Contrastive dual gating: Learning sparse features with contrastive learning. In *2022 IEEE/CVF Conference on Computer Vision and Pattern Recognition (CVPR)*, pp. 12247–12255, 2022. doi: 10.1109/CVPR52688.2022.01194. 1, 4
- Mishra, A. and Marr, D. Apprentice: Using knowledge distillation techniques to improve low-precision network accuracy. *arXiv preprint arXiv:1711.05852*, 2017. 3
- Oord, A. v. d., Li, Y., and Vinyals, O. Representation learning with contrastive predictive coding. *arXiv preprint arXiv:1807.03748*, 2018. 3
- Pan, S., Qin, Y., Li, T., Li, X., and Hou, L. Momentum contrastive pruning. In *2022 IEEE/CVF Conference on Computer Vision and Pattern Recognition Workshops (CVPRW)*, pp. 2646–2655, 2022. doi: 10.1109/CVPRW56347.2022.00298. 4
- Tian, Y., Krishnan, D., and Isola, P. Contrastive representation distillation. In *International Conference on Learning Representations*, 2019. 1, 4
- Tian, Y., Sun, C., Poole, B., Krishnan, D., Schmid, C., and Isola, P. What makes for good views for contrastive learning? *Advances in Neural Information Processing Systems*, 33:6827–6839, 2020. 3
- Tiwari, R., Bamba, U., Chavan, A., and Gupta, D. Chipnet: Budget-aware pruning with heaviside continuous approximations. In *International Conference on Learning Representations*, 2020. 3
- Veit, A. and Belongie, S. Convolutional networks with adaptive inference graphs. In *Proceedings of the European Conference on Computer Vision (ECCV)*, pp. 3–18, 2018. 1, 2, 3, 4, 5
- Wang, X., Yu, F., Dou, Z.-Y., Darrell, T., and Gonzalez, J. E. Skipnet: Learning dynamic routing in convolutional networks. In *Proceedings of the European Conference on Computer Vision (ECCV)*, pp. 409–424, 2018. 3
- Wu, W., He, D., Tan, X., Chen, S., Yang, Y., and Wen, S. Dynamic inference: A new approach toward efficient video action recognition. In *Proceedings of the IEEE/CVF Conference on Computer Vision and Pattern Recognition Workshops*, pp. 676–677, 2020. 3
- Wu, Z., Nagarajan, T., Kumar, A., Rennie, S., Davis, L. S., Grauman, K., and Feris, R. Blockdrop: Dynamic inference paths in residual networks. In *Proceedings of the IEEE Conference on Computer Vision and Pattern Recognition (CVPR)*, June 2018a. 3
- Wu, Z., Xiong, Y., Yu, S. X., and Lin, D. Unsupervised feature learning via non-parametric instance discrimination. In *Proceedings of the IEEE conference on computer vision and pattern recognition*, pp. 3733–3742, 2018b. 3
- Xu, G., Liu, Z., Li, X., and Loy, C. C. Knowledge distillation meets self-supervision. In *European Conference on Computer Vision*, pp. 588–604. Springer, 2020. 4
- You, Y., Gitman, I., and Ginsburg, B. Large batch training of convolutional networks. *arXiv preprint arXiv:1708.03888*, 2017. 5
- Yu, J., Yang, L., Xu, N., Yang, J., and Huang, T. Slimmable neural networks. In *International Conference on Learning Representations*, 2019. URL <https://openreview.net/forum?id=HlgMCsAqY7>. 5, 8
- Zbontar, J., Jing, L., Misra, I., LeCun, Y., and Deny, S. Barlow Twins: Self-Supervised Learning via Redundancy Reduction. 2021. 3, 7
- Zhang, T., Ye, S., Zhang, K., Tang, J., Wen, W., Fardad, M., and Wang, Y. A systematic dnn weight pruning framework using alternating direction method of multipliers. In *Proceedings of the European Conference on Computer Vision (ECCV)*, pp. 184–199, 2018. 4

A. Additional Implementation Details.

A.1. Data Augmentation

We follow the augmentation strategy as outlined in VICReg (Bardes et al.) which remains a standard augmentation strategy in current SSL scenario. The following augmentations were applied sequentially:

- Random cropping with an area uniformly sampled with size ratio between 0.2 to 1.0, followed by resizing to size (224×224), (32,32), (96,96) for ImageNet-100, CIFAR-10/100 and STL-10 respectively.
- Random horizontal flip with probability 0.5.
- Color jittering of brightness, contrast, saturation and hue, with probability 0.8. ColorJitter(0.4, 0.4, 0.2, 0.1) in PyTorch.
- Grayscale with probability 0.2.
- Solarization with probability 0.1.
- Color normalization varies for different datasets:
 1. STL-10/CIFAR-10: mean = (0.4914, 0.4823, 0.4466), std = (0.247, 0.243, 0.261).
 2. ImageNet-100: mean = (0.485, 0.456, 0.406), std = (0.228, 0.224, 0.225).
 3. CIFAR-100: mean = (0.5071, 0.4865, 0.4409), std = (0.2673, 0.2564, 0.2762)

A.2. Pseudocode

For an elaborate and clear understanding of our proposed setting, PyTorch-style pseudocode has been described in Algorithm 1. The value of the `flag` parameter determines whether dense (`flag=1`) or gated (`flag=0`) computation should be performed.

A.3. Channel Selection

For channel selection, we follow the approach proposed in the work of (Li et al., 2021). Figure 3 highlights modified (gated) form of ResNet-18 (He et al., 2016) basic block. The channel gating modules have been inserted between the two convolutions in the basic blocks.

Figure 4 depicts the entire pipeline for channel selection during a forward (dashed arrow) and backward pass (arrow). During training binary mask m is directly multiplied to the activated output of convolutional layers whereas during inference m denotes input sparsity of later layer or output sparsity of previous layer. Gumbel-softmax trick (Jang et al., 2016) is used to ensure that the computational graph is not broken during backpropagation due to non-differentiable discrete channel selection process.

Algorithm 1 Pytorch-style pseudocode

```
#D: Cifar100.
#f_theta: base encoder (ResNet18).
#g_phi: expander MLP.
#L_VICReg: Equation 1.
#L_G: Equation 3.
#flag = 0/1; to set gates on/off
#t_d: Target budget.

for x in data_loader():
    #transformed views
    x1 = Transform(x) # (B, 3, 32, 32)
    x2 = Transform(x) # (B, 3, 32, 32)
    #forward pass
    o1 = f_theta(x1, t_d, flag=0) #gated comp.
    o2 = f_theta(x2, flag=1) #dense comp.
    #o1, o2: type dict()
    f1 = o1["feats"] # (B, 512)
    f2 = o2["feats"] # (B, 512)
    e1 = g_phi(f1) # (B, 2048)
    e2 = g_phi(f2) # (B, 2048)
    #get layer-wise flops
    fr = o1["f_l^R"] #gated-flops
    fo = o1["f_l^O"] #Original-flops
    #loss calculation
    L_G = sparsity_loss(fr, fo, t_d, lambda)
    L_VICReg = ssl_loss(e1, e2, mu, nu, eta)
    #total loss
    loss = L_G + L_VICReg
    #optimization step
    loss.backward()
    optimization.step()
```

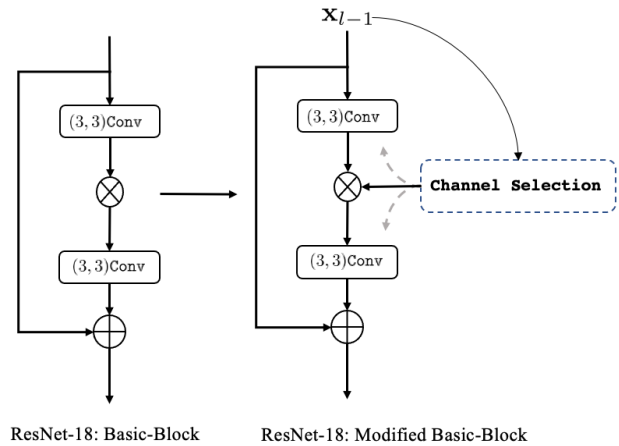


Figure 3. Application of Channel Gating to ResNet-18 **Basic Block**. Dashed arrows represent inference route

